

Perturbed-Angular-Correlation Study of Electric-Quadrupole Interactions in ^{172}Yb in Thulium Metal and Oxide Lattices*

R. L. RASERA AND A. LI-SCHOLZ

Department of Physics, University of Pennsylvania, Philadelphia, Pennsylvania 19104

(Received 16 October 1969)

Electric-quadrupole hyperfine interactions at ytterbium ions in thulium metal and Tm_2O_3 have been investigated at 296°K using time-differential perturbed angular correlation in γ -ray cascades in ^{172}Yb . The ratio of the spectroscopic quadrupole moments of the 1174- and 79-keV states in ^{172}Yb was measured to be $Q(1174)/Q(79) = 1.33 \pm 0.15$. Using this ratio and a value for $Q(79)$ obtained from the Coulomb-excitation transition probability, the magnitudes of the electric-field-gradient (EFG) tensors are obtained. For ytterbium in thulium metal, the measured quadrupole interaction frequencies in the respective nuclear states are found to be $\omega_0(1174) = (101 \pm 4) \times 10^6$ rad/sec, $\omega_0(79) = (190 \pm 19) \times 10^6$ rad/sec, yielding for the magnitude of the largest component of the field gradient $V_{zz} = (4.53 \pm 0.47) \times 10^{17}$ V/cm² at 296°K, a value not significantly different from that found at thulium nuclei in thulium metal, indicating no significant ionic contribution to the EFG. In thulium sesquioxide, the corresponding values for the C_2 site are $\omega_0(1174) = (374 \pm 30) \times 10^6$ rad/sec and $\omega_0(79) = (701 \pm 56) \times 10^6$ rad/sec, from which $V_{zz} = (1.67 \pm 0.20) \times 10^{18}$ V/cm². The anisotropy η expected from crystal-symmetry considerations is not observable within the experimental accuracy, and is probably small. The half-life of the 79-keV state in ^{172}Yb was measured to be 1.80 ± 0.05 nsec. Within the time range of the experiment, no time-dependent attenuations or aftereffects of preceding decay events were found.

I. INTRODUCTION

THE study of electric-quadrupole (EQ) interactions between the atomic nucleus and its environment in the rare-earth elements is of benefit to both solid-state and nuclear physics. In solids, it provides insight into the nature and symmetry of crystalline fields, both directly and through their effect on the electronic structure of the atom. Information can also be obtained concerning nuclear electric-quadrupole moments. In recent years, several studies of electric-quadrupole hyperfine interactions have been made in various rare-earth ions and lattices using the technique of nuclear γ -ray resonance (the Mössbauer effect). In particular, the element thulium has received considerable attention because of the existence of an excellent Mössbauer state, the 8.4-keV state in ^{169}Tm , as well as the availability of both theoretical and experimental information concerning thulium ions and crystals.¹⁻⁶ The present work uses the time-differential perturbed angular correlation (PAC) of nuclear γ rays to investigate the properties of ytterbium as an impurity in thulium metal and oxide matrices. In such a system, it is expected that the direct contribution of the crystal field to the electric field gradient (EFG)

at the nuclear site will be substantially that observed in corresponding thulium compounds, while the ionic contributions will be those characteristic of the ytterbium ion in that lattice. PAC measurements and Mössbauer "source" experiments are better suited to such impurity investigations than are the usual Mössbauer "absorber" experiments (i.e., where the substance under study is the absorber). PAC has the additional advantage of applicability to a class of radioisotopes different from, although overlapping, the Mössbauer nuclides; also PAC is useful at elevated temperatures where recoilless fractions become unusably small in all but a few Mössbauer isotopes. However, these experiments are often difficult, both to perform and to interpret. Nevertheless, such measurements have yielded good results in favorable cases.⁷⁻⁹

The isotope studied in these experiments, ^{172}Yb , has several characteristics that make it a good candidate for time-differential PAC investigations. It possesses two γ -ray cascades that have very large anisotropies, and which proceed through states with lifetimes in the range of 10^{-8} – 10^{-9} sec. This time is comparable to the best instrumental time resolution attainable with NaI(Tl) scintillators at the relevant energies. It is also of the same order as $(\omega_0)^{-1}$, the characteristic precession time for the magnitude of the quadrupole interaction expected in this case. In this paper we present results of measurements of the ratio of the EQ moments of the 1174-keV nuclear state to that of the 79-keV nuclear state, the lifetime of the 79-keV level, and the

* Work supported in part by the U. S. Army Research Office (Durham) and by the U. S. Office of Naval Research.

¹ M. Kalvius, W. Wiedemann, R. Koch, P. Kienle, and H. Eicher, *Z. Physik* **170**, 267 (1962).

² R. L. Cohen, U. Hauser, and R. L. Mössbauer, in *Proceedings of the Second International Conference on the Mössbauer Effect*, edited by D. M. J. Compton and A. H. Schoen (John Wiley & Sons, Inc., New York, 1962).

³ R. G. Barnes, R. L. Mössbauer, E. Kankleit, and J. M. Poindexter, *Phys. Rev.* **136**, A175 (1964).

⁴ D. L. Ührich and R. G. Barnes, *Phys. Rev.* **164**, 428 (1967).

⁵ J. B. Gruber, W. F. Krupke, and J. M. Poindexter, *J. Chem. Phys.* **41**, 3363 (1964).

⁶ R. M. Sternheimer, M. Blume, and R. F. Peierls, *Phys. Rev.* **173**, 376 (1968).

⁷ R. W. Sommerfeldt, T. W. Cannon, L. W. Coleman, and L. Schechter, *Phys. Rev.* **138**, B763 (1965).

⁸ P. da R. Andrade, A. Maciel, and J. D. Rogers, *Phys. Rev.* **159**, 196 (1967).

⁹ R. M. Lieder, W. Delang, and M. Fleck, in *Hyperfine Structure and Nuclear Radiations*, edited by E. Matthias and D. A. Shirley (North-Holland Publishing Co., Amsterdam, 1968), p. 404.

application of time-differential PAC in these states to an investigation of the EFG tensors in metal and oxide lattices at room temperature. A portion of these results has already been reported elsewhere.¹⁰

II. THEORY

In this section we give a brief summary of the theory of electric-quadrupole interactions, and the application of PAC to their study. A number of review articles have treated both the former^{11,12} and the latter¹³ subjects in detail. The Hamiltonian for the EQ hyperfine interaction between a nucleus of spin I and spectroscopic quadrupole moment Q and the EFG tensor of its environment $[V_{ij}]$ can be written in principal axes of the EFG tensor as

$$H_{EQ} = \frac{eQ}{4I(2I-1)} \times [V_{zz}(3I_z^2 - I^2) + \frac{1}{2}(V_{xx} - V_{yy})(I_+^2 + I_-^2)]. \quad (1)$$

In lattices of sufficiently high symmetry, a system can be found where $V_{xx} = V_{yy}$, and in this axially-symmetric case, only one parameter, V_{zz} , is needed to specify the characteristics of the system since Laplace's equation must also be satisfied. The components of the EFG tensor contain contributions from the direct crystalline field and from the unfilled $4f$ shell, with the appropriate shielding^{6,14} of each contribution by distortion of closed shells:

$$V_{ii} = (1 - \gamma_\infty) V_{ii}^{(\text{lat})} + (1 - R) \langle V_{ii}^{(4f)} \rangle_T. \quad (2)$$

In the case of metals, a further term is added to include the direct EFG contribution from the conduction electrons.⁴ The lattice contribution is related to the lattice-sum coefficients A_n^m which appear in the interaction Hamiltonian of the rare-earth ion in a crystalline electric field (CEF), which can be written in the form of a sum on i over the $4f$ electrons:

$$3\mathcal{C}_{\text{CEF}} = \sum_i \sum_{n,m} A_n^m r_i^n Y_n^m(\theta_i, \varphi_i). \quad (3)$$

The direct contributions from the lattice are related to the equivalent order lattice-sum term:

$$V_{zz}^{(\text{lat})} = -4A_2^0/e, \\ V_{xx}^{(\text{lat})} - V_{yy}^{(\text{lat})} = -4A_2^2/e.$$

The contribution from the unfilled $4f$ shell, on the

other hand, depends on the splitting of the ionic energy levels by the Hamiltonian of the crystalline field. It can be calculated, if the lattice parameters are known, by diagonalizing the matrix of the Hamiltonian (3) in the free-ion $|nLJM\rangle$ representation, thus obtaining the set of eigenfunctions $|\nu\rangle$ and the splitting of the J manifold concerned. This procedure is simplified if the excited J manifolds are sufficiently far away in energy for their influence to be negligible, as is the case for Yb^{3+} . To find the field gradient, the matrix elements of the quadrupole operators, e.g., $\langle \nu | 3J_z^2 - J(J+1) | \nu \rangle$, are formed. The resultant EFG at the nucleus is a Boltzmann average over the contributions of the several ionic levels. Thus, although both the direct crystal-field and ionic terms are determined by the CEF parameters A_n^m , the former is to lowest order independent, the latter, strongly dependent on temperature.

The CEF parameters can be calculated from lattice sums; however, the difficulty of such a calculation is considerable, and the results are in rather poor agreement with observation.¹⁵ Experimentally, these parameters may be obtained from optical spectra by a computer fitting procedure, which takes into account the positions of several multiplets. This has been done for oxides of erbium and thulium by Gruber, Krupke, and Poindexter.⁵ It is convenient to include the radial moment and the lattice-sum parameter in a common term C_n^m , which can be fit from experimental data alone. This term is defined by the relation

$$C_n^m = A_n^m \langle r^n \rangle_{4f} (1 - \sigma_n),$$

where the term $(1 - \sigma_n)$ takes into account the shielding of the $4f$ shell from the crystal field by the closed $5s$ and $5d$ shells, which lie largely outside the $4f$ shell. The shielding factor σ_n is found^{6,15} to be important only for $n=2$.

The application of time-differential PAC to the investigations of static EQ interactions is made via the perturbation factors $G_k(t)$ that appear in the expression for the angular and temporal γ -ray distribution functions

$$W(\theta, t) = 1 + \sum_k G_k(t) A_k P_k(\cos\theta). \quad (4)$$

$W(\theta, t)$ gives the probability that the second γ ray of a cascade will be emitted at an angle between θ and $\theta + d\theta$ with respect to the emission direction of, and within a time interval $(t, t+dt)$ following the first γ ray of the cascade. The sum is over even k , usually up to a maximum value of $k=4$. A_k is the unperturbed angular correlation coefficient, dependent only on the spins and structure of the nuclear states involved in the cascade, and $P_k(\cos\theta)$ is a Legendre polynomial. All extranuclear effects are carried in the factors $G_k(t)$. These perturbation factors describe the change in the state of polarization of the nucleus through interaction

¹⁰ A. Li-Scholz and R. L. Rasera, Phys. Rev. Letters **23**, 181 (1969).

¹¹ R. L. Mössbauer, Rev. Mod. Phys. **36**, 362 (1964).

¹² S. Ofer, I. Nowik, and S. G. Cohen, in *Chemical Applications of Mössbauer Spectroscopy*, edited by V. I. Goldanskii and R. H. Herber (Academic Press Inc., New York, 1968), Chap. 8.

¹³ H. Frauenfelder and R. M. Steffen, in *Alpha-, Beta-, and Gamma-Ray Spectroscopy*, edited by K. Siegbahn (North-Holland Publishing Co., Amsterdam, 1965), Vol. 2, Chap. XIX A.

¹⁴ R. M. Sternheimer, Phys. Rev. **146**, 140 (1966), and references cited therein.

¹⁵ G. Burns, J. Chem. Phys. **42**, 377 (1965).

with the environment during the time, that the nucleus is in the intermediate state of the gamma cascade; thus $G_k(t)$ depends on the nuclear moments and spin I of this state only. In the case of static interactions $G_k(t)$ has oscillatory behavior, the exact functional form depending on the character of the interaction. In polycrystalline samples, $G_k(t)$ has a particularly simple form for static EQ interactions if the field gradient possesses axial symmetry.¹⁶ Then

$$G_k(t) = \sum_n s_{kn} \cos(n\omega_0 t), \quad (5)$$

where the s_{kn} are sums of angular-momentum vector addition coefficients

$$s_{kn} = \sum_{m, m'} \begin{pmatrix} I & I & k \\ m' & -m & m-m' \end{pmatrix}$$

with $|m^2 - m'^2| = n$ for integer, $\frac{1}{2}n$ for half-integer I . The quadrupole frequency is defined¹³ for integer I to be

$$\omega_0 = -\frac{3eQV_{zz}}{4I(2I-1)}. \quad (6)$$

When the symmetry is lower than axial, $G_k(t)$ loses its simple periodic form, and must be calculated numerically. This was first done by Matthias, Schneider, and Steffen¹⁷ in terms of V_{zz} and the asymmetry parameter $\eta = (V_{xx} - V_{yy})/V_{zz}$. The results of a calculation of $G_k(t)$ for intermediate nuclear spins $I=2$ and 3 , the cases of interest for ^{172}Yb , are presented in an Appendix to this paper for a range of EFG asymmetries. In the event that the fields observed at the nucleus vary with time, there will in general be a further attenuation due to loss of orientation of the ensemble of nuclei in the intermediate state. Abragam and Pound¹⁶ showed that in the limit of weak and rapidly varying fields, an exponential dropoff of the anisotropy with time is to be expected. Recent, less restricted calculations by Blume and Tjon¹⁸ and Blume¹⁹ confirm this general trend.

III. EXPERIMENT

Observation of time-differential PAC involves recording the angular distribution of the second γ ray in a nuclear cascade with respect to the direction of the first, as a function of the time interval between, which is the time spent in the intermediate nuclear state. The time-and-angle spectrometer used in this experiment is built on a circular table with the angle between the two γ -ray detectors variable over the range 90° – 270° . A $1\frac{1}{2}$ -in. \times $1\frac{1}{2}$ -in. NaI(Tl) scintillator is used to detect the high-energy γ ray, while a $\frac{1}{4}$ -in. \times 2-in. crystal of the

same material is used in the low-energy channel. Both detectors are optically coupled to RCA-8575 photomultiplier tubes. Each tube feeds conventional "slow" linear and coincidence circuitry, and also a "fast" time spectrometer. The latter consists of a wide-band amplifier (in the low-energy channel only), fast discriminators for leading-edge timing, and a time-to-amplitude converter (TAC). The pulse-height distribution at the output of the TAC represents the distribution of time intervals between the arrival of pulses from the two detectors. This pulse-height distribution is stored in a multichannel pulse-height analyzer gated by the "slow" coincidences.

The decay of 6.7-day ^{172}Lu to ^{172}Yb , shown in part in Fig. 1, has been studied by many authors,^{20–23} and the major features of the decay scheme are now well understood. Of interest for PAC studies are the cascades

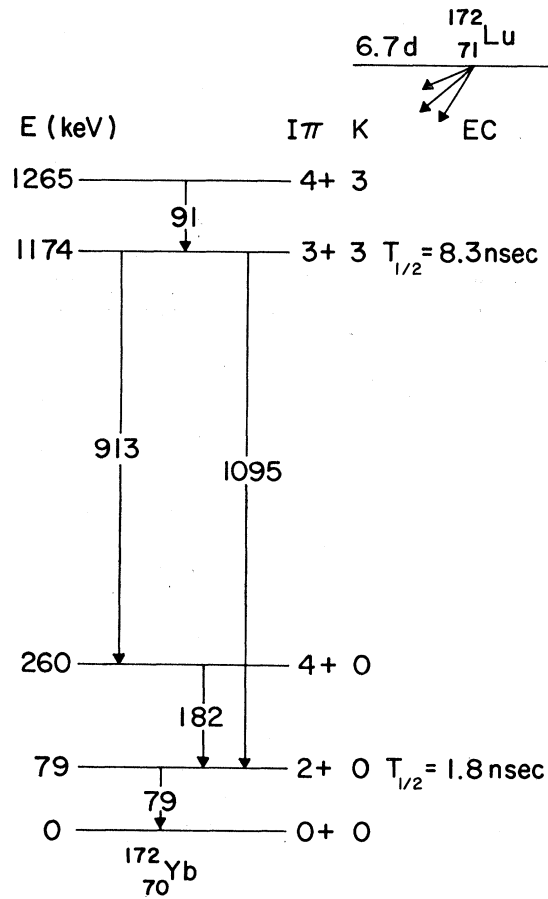


FIG. 1. Relevant portion of the decay scheme of ^{172}Lu to ^{172}Yb .

²⁰ B. Harmatz, T. H. Handley, and J. W. Mihelich, Phys. Rev. **123**, 1758 (1961).

²¹ H. Blumberg, K.-H. Speidel, H. Schlenz, P. Weigt, H. Hübel, P. Göttel, H.-F. Wagner, and E. Bodenstedt, Nucl. Phys. **A90**, 65 (1967).

²² P. Kleinheinz, R. Vukanovic, M. Zupancic, L. Samuelsson, and H. Lindström, Nucl. Phys. **A91**, 329 (1967).

²³ Geoffrey Kaye, Nucl. Phys. **A108**, 625 (1968).

¹⁶ A. Abragam and R. V. Pound, Phys. Rev. **92**, 943 (1953).

¹⁷ E. Matthias, W. Schneider, and R. M. Steffen, Phys. Letters **4**, 41 (1963).

¹⁸ M. Blume and J. A. Tjon, Phys. Rev. **165**, 446 (1968).

¹⁹ M. Blume, in *Hyperfine Structure and Nuclear Radiations*, edited by E. Matthias and D. A. Shirley (North-Holland Publishing Co., Amsterdam, 1968), p. 911.

TABLE I. Characteristics of relevant γ -ray cascades in the decay of ^{172}Lu to ^{172}Yb . The half-lives and spectroscopic quadrupole moments given refer to the intermediate states of the respective cascades.

Cascade energies keV	Spin sequence	Half-life nsec	Angular correlation coefficients ^a A_2 A_4		Quadrupole moment barns
91-1095	$4^+ - 3^+ - 2^+$	8.3 ± 0.3^b	$+0.42 \pm 0.02$	$+0.012 \pm 0.025$	2.92 ± 0.33^c
1095-79	$3^+ - 2^+ - 0^+$	1.80 ± 0.05^c	-0.41 ± 0.01	-0.042 ± 0.012	2.21 ± 0.06^d

^a Reference 21.^b *Nuclear Data Sheets*, compiled by K. Way *et al.* (U. S. Government Printing Office, National Academy of Sciences-National Research Council, Washington, D. C. 20025).^c Present work.^d Reference 24.

$(4^+)91(3^+)1095(2^+)$ and $(3^+)1095(2^+)79(0^+)$. These cascades are found to have very large anisotropies. Furthermore, both intermediate states possess lifetimes of the order of nanoseconds. A summary of the properties of these cascades, taken from the Nuclear Data Sheets and Refs. 21, 22, and 24 is given in Table I. The fortuitous placement of these transitions in the decay scheme allows the time spectrum of both cascades to be stored simultaneously. The 1095-keV γ ray is common to both spectra, being the second member of the first cascade and the first member of the second. Moreover, the 79- and 91-keV lines are sufficiently close together to be included in a common single-channel window. If these low-energy lines are chosen to generate the “start” pulse to the TAC, and the 1095-keV γ ray, with suitable delay inserted, the “stop” pulse, then the time distribution of the 91-1095 keV spectrum appears to the high-pulse-height side of that amplitude corresponding to zero time, and that of the 1095-79-keV cascade, to the low side. It should be pointed out that, aside from the small shift in triggering time due to the difference in energy between the 79- and 91-keV lines, the zero point in time is the same for both spectra, independent of other instrumental effects. The price paid for this useful characteristic is in the requirement of a rather wide single-channel window ($\Delta E/E \approx 25\%$) in the 79/91-keV channel, leading to a deterioration of the time resolution attainable using leading-edge timing. The full width at half maximum of the prompt peak, measured with a Co^{60} source but with energy windows set as in the ^{172}Yb experiment was 2.3 nsec, with slopes of 0.55 nsec and 0.42 nsec for the “early” and “late” sides of the prompt curve. The “true” prompt for the 91-1095- and 1095-79-keV cascades would be slightly different from each other, and presumably better than this composite prompt spectrum.

In order to produce ^{172}Lu in a thulium lattice, the radioactive samples were prepared by the $^{169}\text{Tm}(\alpha, n)$ reaction using the Heavy Ion Linear Accelerator at Yale University. This method of production has the added advantage that separated isotopes are not needed since ^{169}Tm is isotopically 100% abundant. The bombarding energy of 21 MeV, chosen to give a reasonable

yield of ^{172}Lu , is above the threshold for the $(\alpha, 2n)$ reaction, and a small amount of ^{171}Lu was also produced. The decay scheme of ^{171}Lu has no γ rays higher in energy than 854 keV, and thus no direct interference with the cascades of interest occurs. However, the existence of copious quantities of x rays accompanying the electron-capture decays of both ^{171}Lu and ^{172}Lu necessitated the use of substantial amounts of absorber in front of each detector (lead and copper for the high-energy, copper for the low-energy side) in order to reduce the integral count rate in each detector. This consideration was the effective limitation on usable source strength.

In cascades in which the anisotropy is primarily $P_2(\cos\theta)$, the effects of the perturbation will be most pronounced at that angle where $P_2(\cos\theta)$ is maximum, i.e., $\theta = 180^\circ$. For this reason, the greater part of our data was taken at that angle, and the fits of $G_2(t)$ were made with this data. Runs were made at 90° in order to assure that the structure seen at 180° was anticorrelated with that at 90° , and also at 135° where $W(\theta) \approx 1$ for both cascades, in order to assure the absence of nonlinearities in the lifetime curves.

IV. LIFETIME OF 79-keV STATE

In extracting the time spectrum of $G_k(t)$ from the raw data, an accurate knowledge of the lifetimes of the nuclear states involved is required. In fitting our data from the 3^+ , 1174-keV state, using a weighted average of the published lifetimes for this state yielded satisfactory results. A similar procedure was attempted for the 2^+ , 79-keV state, but a good fit could not be obtained. This, coupled to the fact that the stated errors in the several recent experimental determinations of this lifetime^{23,25-28} are generally smaller than the scatter of the values, motivated a remeasurement of the lifetime of the 79-keV state.

²⁵ C. Günther, W. Engels, and E. Bodenstedt, *Phys. Letters* **10**, 77 (1964).

²⁶ J. W. Tippie and R. P. Scharenberg, *Phys. Rev.* **141**, 1062 (1966).

²⁷ P. Kleinheinz and J. Braunsfurth, private communication to A. Märelus, P. Sparrmann, and T. Sundström, quoted in *Hyperfine Structure and Nuclear Radiations*, edited by E. Matthias and D. A. Shirley (North-Holland Publishing Co., Amsterdam, 1968), Appendix D.

²⁸ R. A. Belt, H. W. Kugel, J. M. Jaklevic, and E. G. Funk, *Nucl. Phys.* **A134**, 225 (1969).

²⁴ B. Elbek, M. C. Olesen, and O. Skilbreid, *Nucl. Phys.* **19**, 523 (1960).

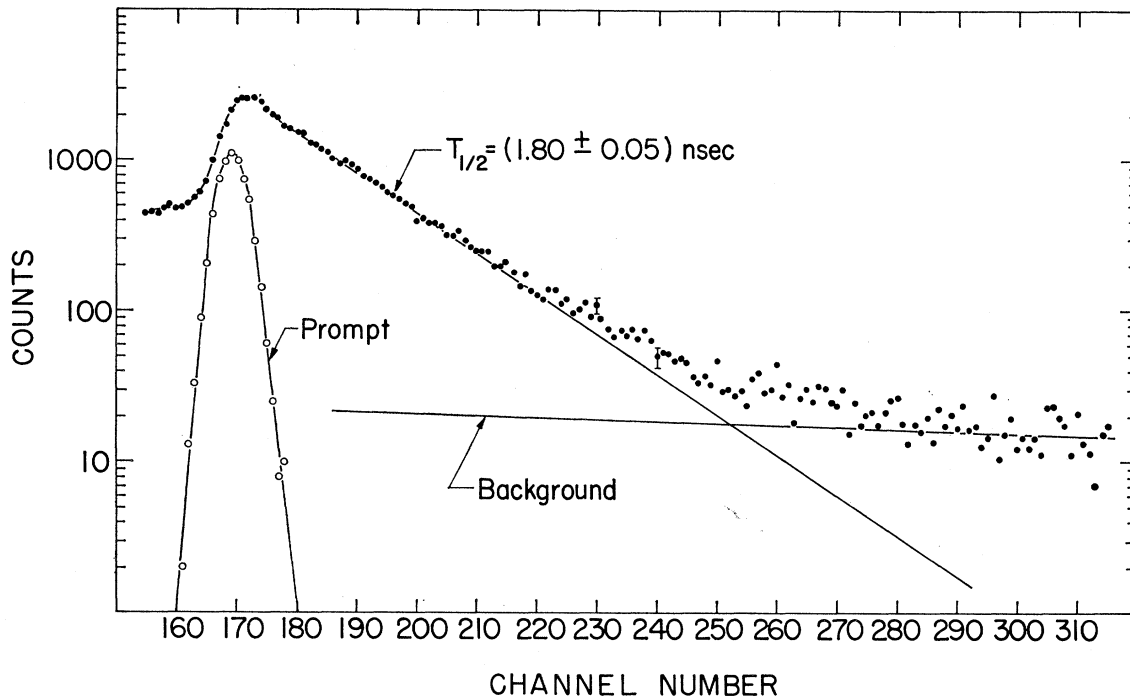


FIG. 2. Half-life measurement of 79-keV state in ^{173}Yb . This data was taken using γ - e^- coincidence in 128° geometry. The background subtracted from the spectrum is composed of random coincidences and also a small contribution from the triple cascade 1114-(1095)-79 keV, which at times longer than a few nanoseconds decays with the 8.3-nsec lifetime of the 1174-keV state.

Three different methods were used for the determination of this lifetime: (1) The same configuration as in the PAC measurement was used at a table angle of 128° , where the angular correlation of the 1095-79-keV cascade is approximately unity (2) Measuring γ - e^- delayed coincidences with conversion electrons from the 79-keV transition detected with a NATON-136 plastic scintillator of 1 mm thickness, again in 128° geometry (Fig. 2). (3) γ - e^- delayed coincidence in essentially 2π "close-up" geometry, with the source sandwiched between the two detectors. All three measurements were made with thulium-metal sources. The performance of the γ -electron coincidence array was 8.7×10^{-10}

sec FWHM, with slopes of 1.15×10^{-10} and 1.30×10^{-10} sec. The time-delay standards used in this experiment were checked against a commercial (ORTEC) calibrated delay box, and against a 50-nsec variably tapped strip line accurate to ± 10 psec, using a sampling oscilloscope in Lissajous mode.²⁹ Both methods yielded essentially the same calibration. As seen in Table II, the results of all three of our half-life measurements are in agreement with one another. A weighted average of three measurements yields a value for $T_{1/2}$ of the 79-keV level of 1.80 ± 0.05 nsec. The greater part of the remanent error is due to systematic uncertainties such as system nonlinearities and drift. Our half-life is some-

TABLE II. Recent lifetime measurements on the 79-keV state in ^{173}Yb . In the column "Method," DC denotes delayed coincidence.

Reference	Method	$T_{1/2}$ (nsec)
Günther <i>et al.</i> ^a	γ - γ DC	1.57 ± 0.04
Tippie and Scharenberg ^b	Coulomb-excitation, pulsed beam	1.70 ± 0.05
Kleinheinz and Braunsfurth ^c	e^- - e^- DC	1.67 ± 0.03
Kaye ^d	γ - e^- DC	1.6 ± 0.4
Belt <i>et al.</i> ^e	γ - e^- DC	1.58 ± 0.06
Funk ^f	γ - γ DC, 125° between detectors.	1.76 ± 0.06
	γ - e^- DC, 125° between detectors.	1.68 ± 0.06
	γ - e^- DC, 2π geometry.	1.64 ± 0.05
Present work	γ - γ DC, 128° between detectors.	1.80 ± 0.07
	γ - e^- DC, 128° between detectors.	1.79 ± 0.06
	γ - e^- DC, 2π geometry.	1.82 ± 0.09
	Weighted average of present work.	1.80 ± 0.05

^a Reference 25.
^b Reference 26.

^c Reference 27.
^d Reference 23.

^e Reference 28.
^f Reference 30.

²⁹ We are grateful to Dr. E. W. Beier for making this equipment available to us at the Princeton-Pennsylvania Accelerator.

what longer than previous measurements, although in fair agreement with that of Tippie and Scharenberg²⁶ and the latest results of Funk.³⁰ It may be that the very characteristics that make this nuclide suitable for PAC studies, namely the large anisotropy of the angular correlation, make it difficult to carry out a lifetime measurement without special care for the geometry of the measurement.

V. PAC MEASUREMENTS IN THULIUM METAL

Figure 3 shows the raw data from the measurement of time-dependent PAC of ^{172}Yb in a thulium metal lattice. The attenuation coefficient $G_2(t)$ derived from these data is shown in Fig. 4. Points near zero time were omitted from the fits in order to prevent distortions due to small amounts of prompt admixtures from competing cascades. The fitted curves are those for an attenuation caused by a static randomly oriented EQ interaction with axial symmetry, whose form was first given by Abragam and Pound.¹⁶ Since the crystal structure of thulium metal is hexagonal-close-packed, deviations from axial symmetry are not expected for regular lattice sites. The structure in $G_2(t)$ is sufficiently well spread out so that the resolving time of the time spectrometer is small in comparison; thus the

functional form of $G_2(t)$ is fairly well preserved in the data. In this experiment, the zero point of time is the same for the two spectra. This simplifies data analysis considerably, since knowledge of the positions of this zero and any one structural feature of the attenuation pattern suffices in principle to establish the quadrupole interaction frequency. If several oscillations are visible, as in the 91–1095-keV side of the spectrum, then ω_0 is constrained within very narrow limits. From the fit of $G_2(t)$ to the data, the quadrupole interaction frequencies are found to be

$$\omega_0(1174) = (101 \pm 4) \times 10^6 \text{ rad/sec},$$

$$\omega_0(79) = (190 \pm 19) \times 10^6 \text{ rad/sec}.$$

It is interesting to observe that the periodic nature of the attenuation coefficients is manifest at times up to 30 nsec. Within this range, no effects attributable to time-dependent interactions evidence themselves. There also appears to be a relatively small frequency distribution about the average quadrupole interaction frequency, in contrast to the situation found in Ta^{181} in hafnium metal by Sommerfeldt *et al.*⁷ and by Andrade *et al.*⁸ The effect of such a frequency distribution is to wash out the structure in the time-differential attenuation curves¹⁷; indeed, a very small spread in ω_0 causes

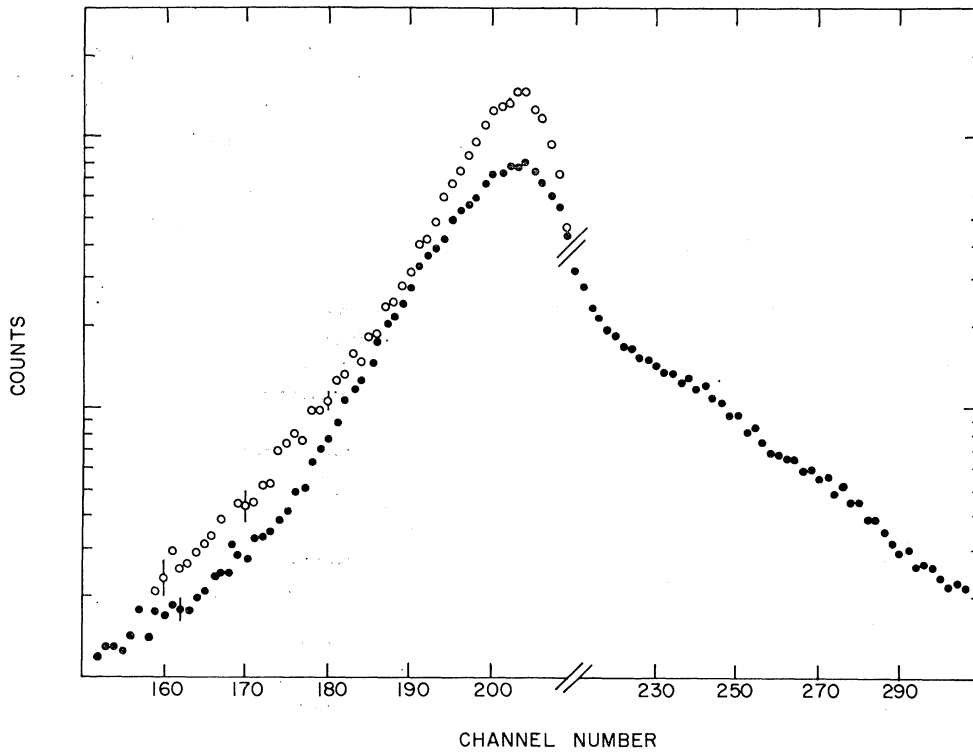


FIG. 3. Time spectrum of the 91–1095 keV (right-hand side) and 1095–79 keV cascades in ^{172}Yb in thulium metal. The data taken at $\theta=90^\circ$ (open circles) is displaced upward slightly from the 180° data (solid circles) for clarity. Note the change in horizontal scale at channel number 213.

³⁰ E. G. Funk (private communication).

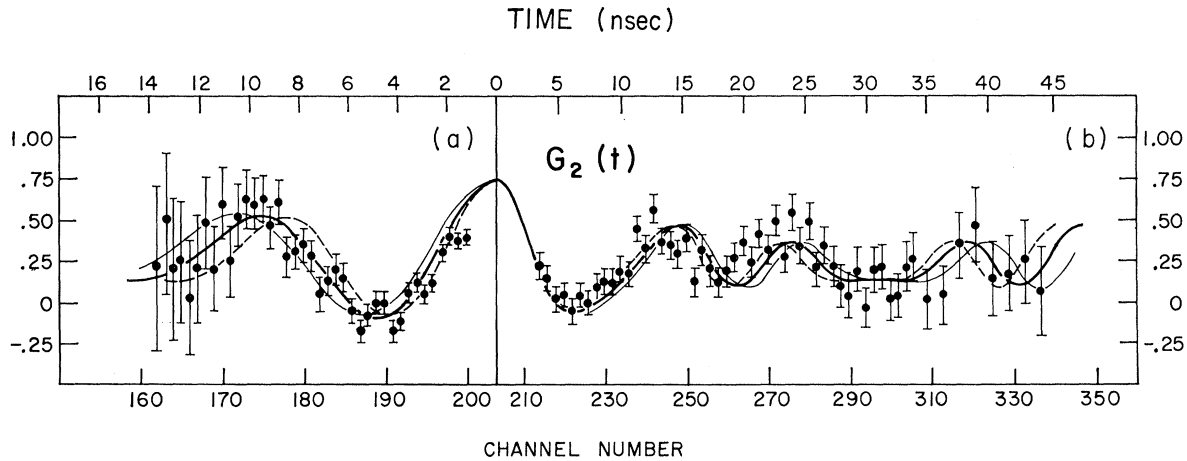


FIG. 4. The time-dependent angular correlation coefficient $G_2(t)$ for (a) the 1095–79 keV cascade and (b) the 91–1095 keV cascade in ^{172}Yb in thulium metal. The heavy solid curve represents the best fit to the data, with the light and broken curves representing the limits of error to the fit [10% in (a) and 4% in (b)]. Since finite time resolution and solid angle effects have not been corrected for, the coefficients $G_2(t)$ are not normalized to unity at $t=0$.

a severe reduction in the effect to be observed. No such reduction is seen within the time range and precision of our experiment. The absence of a spread in the interaction strength indicates also that the effect of lattice imperfections such as those due to strains or to radiation damage effects from the source bombardment is not important at a large majority of the ytterbium sites. This may be due to annealing of such defects in the heat of the day-long bombardment of the sample.

The quadrupole frequency ω_0 involves the product of the nuclear moment and V_{zz} . Under the reasonable assumption that the EFG seen by nuclei undergoing both cascades is the same, the ratio of the static quadrupole moments of the nuclear states involved can be obtained directly and without recourse to model or EFG calculations by forming the ratio of the two frequencies. From (6),

$$\frac{Q(1174)}{Q(79)} = -\frac{5 \omega_0(1174)}{2 \omega_0(79)} = 1.33 \pm 0.15.$$

Wagner and co-workers have recently measured this ratio by a different method.³¹ Using time-differential PAC to investigate the time-dependent attenuation of the angular correlation from ^{172}Yb in a liquid solution, they find a ratio for the spectroscopic moments $Q(1174)/Q(79) = 1.57 \pm 0.23$ based on analysis of the time-dependent interaction according to the theory of Abragam and Pound.¹⁶ This value is in quite good agreement with our result.

The magnitude of the quadrupole moment of the 79-keV state can be calculated from the reduced $E2$ transition probability $B(E2)$ for the ground-state transition under the assumptions of the nuclear collective model. The general applicability of this model

in this (Z, A) region is well established. Using the Coulomb-excitation data of Elbek *et al.*,²⁴ the spectroscopic EQ moment of the 79-keV state is calculated to be $Q(79) = 2.21 \pm 0.06$ b which, combined with the above ratio, yields $Q(1174) = 2.92 \pm 0.33$ b .

With the quadrupole moments known, the magnitude of V_{zz} follows directly: using the lower cascade, e.g.,

$$V_{zz} = 8\hbar\omega_0(79)/eQ(79) = (4.53 \pm 0.47) \times 10^{17} \text{ V/cm}^2$$

for ytterbium in thulium metal at 296°K.

VI. PAC MEASUREMENTS IN Tm_2O_3

The results of the sum of three measurements on ^{172}Yb in thulium oxide are shown in Fig. 5. In several respects this case is much more difficult than that of the metal. The crystal structure is more complex, with two inequivalent rare-earth sites, the more populated of which possesses very low (C_2) symmetry and thus admits the possibility of an anisotropic EFG. Furthermore, the quadrupole frequency observed is considerably higher than in the metal; thus the finite time resolution of the instrument reduces the amplitude of the structure in the time spectrum by a considerable amount. Finally, the oxide targets have a smaller yield of ^{172}Lu , resulting in weaker sources and therefore longer runs, which test severely the long-term stability of the time spectrometer. Nevertheless, some of the salient features of the interaction can be observed in the data. The curves drawn in Figs. 5(b) and 5(c) correspond to a fit to the data of a single symmetric EQ interaction, as in the metal case, with the constraint that the ratio of the interaction frequencies be the same as that found in thulium metal. Only the more populated (C_2) rare-earth site is thereby considered. This is allowable since there are three times as many of these sites as there are of the less-populated sites with C_{3i}

³¹ M. Forker and H. F. Wagner, Nucl. Phys. **A138**, 13 (1969).

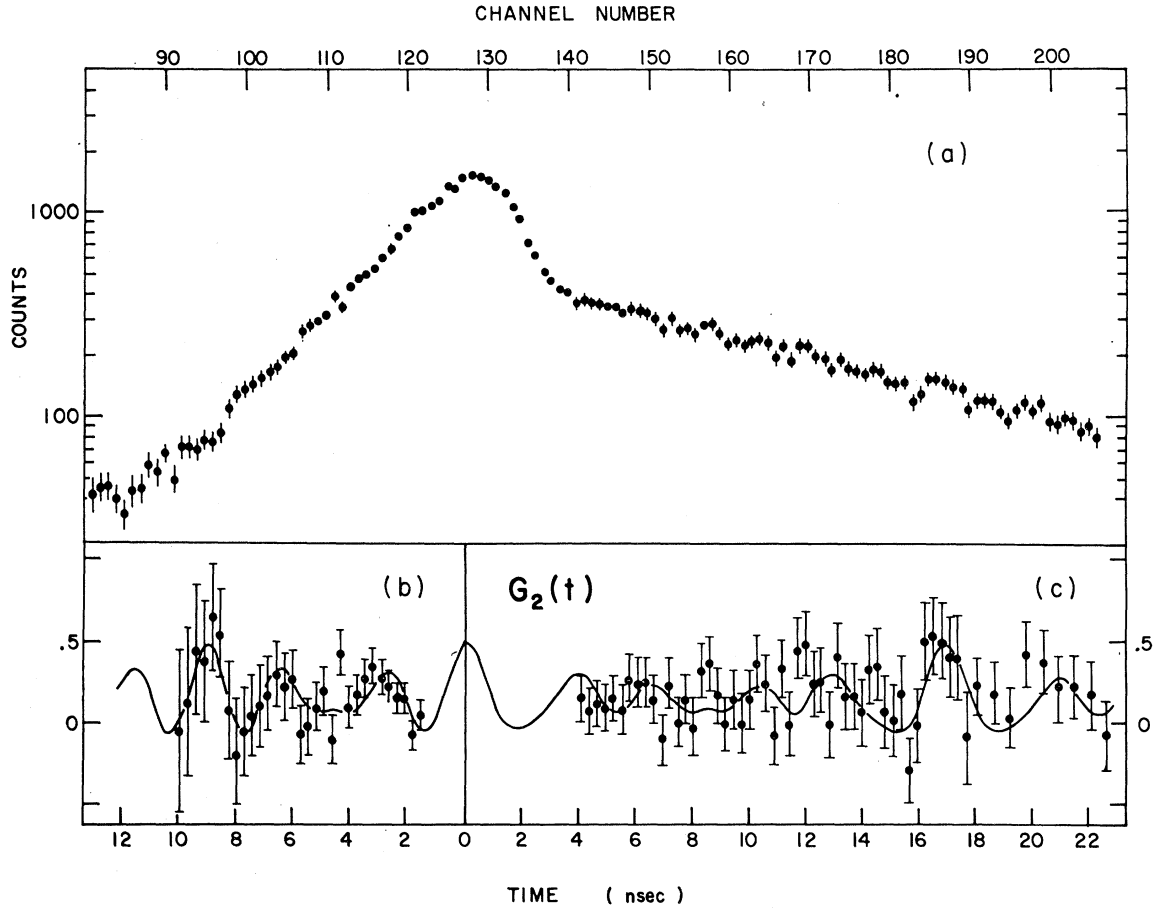


FIG. 5. Results of the measurements on ^{172}Yb in Tm_2O_3 . (a) Time spectrum taken at $\theta = 180^\circ$. Below (a) are shown the corresponding unnormalized attenuation coefficients $G_2(t)$ for (b) the 1095-79-keV cascade, and (c) the 91-1095-keV cascade. The solid curve in (b) and (c) represents a fit to the data using the ratio of the quadrupole interaction frequencies derived from the thulium metal data (see text).

symmetry. Moreover, recent Mössbauer-effect experiments³²⁻³⁴ on various isotopes in ytterbium oxide have shown that the EQ interaction strength of the C_{3i} sites is much smaller than that at the C_2 sites. In terms of $G_2(t)$, this means a slowly varying time dependence upon which the more rapidly fluctuating structure is superimposed. In this case the relative peak heights, but not their positions, will be affected. The same can be said for the effect of the asymmetry of the EFG tensor in the C_2 sites. Mössbauer measurements at temperatures below 77°K yield³²⁻³⁴ an overall asymmetry parameter $\eta \approx 0.1$. From the calculations given in the Appendix it is seen that such a small value of η has no effect on peak position in the first period of oscillation of $G_2(t)$.

The fit thus obtained yields values for the EQ

interaction frequencies of

$$\begin{aligned}\omega_0(1174) &= (374 \pm 30) \times 10^6 \text{ rad/sec}, \\ \omega_0(79) &= (701 \pm 56) \times 10^6 \text{ rad/sec}.\end{aligned}$$

The quality of the fit is adequate, within the statistical accuracy of the data. Here too, there is no evidence of time-dependent interactions. In insulating sources, one might also expect to see aftereffects of preceding decays, which manifest themselves through disturbances in the atomic electron shells. The fact that the data can be fit while requiring the same interaction frequency ratio as in the metal, where such effects are not expected, indicates that the atomic shell recovers from the K -capture decay (or from preceding internal conversion) in a time short compared to the 8.3-nsec half-life of the 1174-keV state. Under the above assumptions, V_{zz} is found to be $(1.67 \pm 0.20) \times 10^{18} \text{ V/cm}^2$ for the Yb^{3+} nucleus at the C_2 site. As mentioned above, no quantitative statement can be made concerning the anisotropy of the EFG except to say that it is certainly small,

³² G. K. Shenoy, B. D. Dunlap, and G. M. Kalvius, *Bull. Am. Phys. Soc.* **14**, 134 (1969); and (private communication).

³³ I. Nowik and S. Ofer, *J. Phys. Chem. Solids* **29**, 2117 (1968).

³⁴ K.-G. Plingen, F.-J. Schröder, and B. Wolbeck (unpublished).

TABLE III. Summary of experimental results on EQ interactions of ^{172}Yb in Tm lattices at 296°K. V_{zz} is calculated using the value for $Q(79)$ of 2.21 ± 0.06 b, obtained from Ref. 24.

Lattice	$\omega_0(1174)$ 10 ⁶ rad/sec	$\omega_0(79)$ 10 ⁶ rad/sec	$Q(1174)/Q(79)$	$eQ(79)V_{zz}$ 10 ⁻⁷ eV	V_{zz} 10 ¹⁷ V/cm ²
Thulium metal	101±4	190±19	1.33±0.15	10±1	4.53±0.47
Tm ₂ O ₃ (C ₂ site)	374±30	701±56	^a	37±4	16.7 ±2.0

^a Quadrupole moment ratio was not calculated for the oxide since it was used as a constraint in the evaluation of the data (see text).

since a large η would have manifested itself by reducing the amplitude of the major peaks at long times, as seen in the Appendix.

VII. DISCUSSION

In rare-earth ions, where the spin-orbit interaction dominates the effect of the crystal field, the total ionic angular momentum J remains a fairly good quantum number in solid lattices. This is especially true for the ions near the ends of the series. The ground-state free-ion configuration of Yb^{3+} is $[\text{Xe}]4f^{13}$, $^2F_{7/2}$; the first excited J -manifold, $^2F_{5/2}$, is approximately 10,000 cm^{-1} removed, and its effect on the ground-state levels can be ignored. Yb^{3+} is a Kramers ion, and thus a hyperfine magnetic field might be expected; however, relaxation of the atomic shell at high temperatures is fast enough so that the nucleus sees a vanishing effective magnetic field. In the divalent ion, ytterbium completes the $4f$ shell, and thus has $J=L=0$. In the following we wish to compare our results for the EFG at the nuclear site to the behavior of these ions in the crystal-line electric fields as obtained from previous experimental data using various models for the interaction. For convenience our results are summarized in Table III.

Thulium metal is a relatively simple case from the standpoint of crystal structure. The lattice symmetry is D_{6h} , and thus only four CEF parameters enter into the potential: A_2^0 , A_4^0 , A_6^0 , and A_6^6 . Uhrich and Barnes performed Mössbauer-effect experiments on the 8.42-keV state in ^{169}Tm in thulium metal, and derived CEF parameters from the temperature dependence of the EQ interaction.⁴ They found the quadrupole splitting above 160°K to be small and relatively temperature-independent, consistent with a vanishing $4f$ contribution to the EFG at high temperatures. The value obtained by Uhrich and Barnes for the total EFG at the nucleus is $V_{zz}=5.16 \times 10^{17}$ V/cm² for temperatures above 160°K. This can be compared to our value for V_{zz} in ytterbium under the assumption that the contribution from the conduction electrons, as well as $\langle r^2 \rangle_{4f}$ and the various shielding factors, do not differ significantly between thulium and ytterbium in comparison with the experimental and theoretical accuracy to which these factors are known.^{6,15,35} Our value of $(4.53 \pm 0.47) \times 10^{17}$ V/cm²

for the high-temperature EFG at ytterbium nuclei in thulium is not substantially different from that found by Uhrich and Barnes for thulium ions in thulium, indicating in our case also that the direct ionic contribution to the EFG is negligible. The $4f$ contribution to the EFG can vanish under either of two circumstances depending on the ionic configuration of the ytterbium impurity. However, the ionic state of ytterbium in thulium metal is not known with certainty. Ytterbium metal crystallizes in an fcc lattice with the individual ions being dipositively charged. If the $2+$ -ionic configuration is maintained when ytterbium is introduced into the hcp thulium lattice, then no direct contribution comes from the closed ionic shells at all. However, it might be argued on the basis of ionic sizes that a Yb^{2+} ion would more easily fit into the thulium lattice than the considerably larger Yb^{3+} ion. If the ionic state is $3+$, the absence of a direct ionic EFG implies that the splitting of the ionic levels in the crystal field is small, so that at elevated temperatures they are essentially equally populated. This is indeed the case in the thulium ions themselves. Uhrich and Barnes found the over-all splitting of the ground-state manifold to be 76 cm^{-1} for thulium metal.⁴ That this splitting should be so small can be explained by observing that the itinerant electrons, in addition to making their own direct contribution to the EFG, also serve to shield the ion from distant lattice points; thus the over-all CEF would be reduced over that expected from straight lattice-sum calculations. There are indications that this is indeed the case. The over-all splitting found by Uhrich and Barnes is much closer to that calculated by Elliott³⁶ using a simplified model in which only nearest neighbors contribute to the field, than it is to the pure lattice-sum value calculated using the planewise-summation method of de Wette.³⁷

In the sesquioxide lattice, there is considerably more experimental information available; however, in view of the complexity of the system, unambiguous interpretation of this mass of data has not been possible. The heavy rare-earth sesquioxides belong to the crystal class T_h .⁷ In this lattice the rare-earth ions are found at two inequivalent sites, populated in the ratio 3:1, with point symmetries C_2 and C_{3i} , respectively. The crystalline field for the more populated site requires no fewer than 14 parameters for its description in the CEF

³⁵ A. J. Freeman and R. E. Watson, Phys. Rev. **127**, 2058 (1962).

³⁶ R. J. Elliott, Phys. Rev. **124**, 346 (1961).

³⁷ F. W. de Wette, Phys. Rev. **123**, 103 (1961).

model. Several Mössbauer-effect measurements using various ytterbium isotopes have recently been made³²⁻³⁴ on Yb_2O_3 , allowing direct comparison with our data. Our result for the magnitude of the EFG at the C_2 site at 296°K is smaller than that found by Shenoy *et al.*³² and by Plingen *et al.*³⁴ at low temperatures. This is to be expected, since the ionic levels are more equally populated at higher temperatures. The absence of gross CEF asymmetry in our data is also in agreement with Mössbauer experiments, all of which find η to be of the order of 0.1. Quantitative comparison of results at different temperatures, however, is not possible due to the absence from the literature of optical-spectrum or other determinations of the Yb^{3+} ionic energy levels and/or wave functions in this lattice. Plingen *et al.* have found³⁴ that the EQ interaction strength remains constant over the entire temperature range below 77°K; this implies that the splitting of the ionic levels is such that the lowest Kramers doublet is separated from the rest of the ground-state J manifold by at least a few hundred wave numbers. However, the reduced value found in the present experiment for the EFG at room temperature makes it unlikely that the separation of the lowest doublet is much more than this amount.

VIII. CONCLUSION

In these experiments, the utility of time-differential PAC as a method for the investigation of EQ hyperfine interaction in the rare-earths has been demonstrated. The previously determined value for the EQ moment of the 79-keV first excited nuclear state in ^{172}Yb has been used to determine the EFG acting at ytterbium nuclei in thulium metal and oxide lattices at 296°K, as well as the EQ moment of the 1174-keV nuclear state. The PAC technique complements that of nuclear γ -ray resonance particularly in that it is applicable at elevated temperatures. This is an especially useful characteristic when investigating EQ interactions in rare-earth ions in solids, since the ionic contribution to the EFG usually dominates the low-temperature EQ interaction, but decreases in importance rapidly with increasing temperature. Thus PAC can be used at high temperatures to single out for study the nonionic contributions to the EFG, i.e., those from the lattice and conduction electrons, and their respective shielding factors. The magnitudes of the EFGs measured in these experiments are consistent with values to be expected on the basis of low-temperature Mössbauer-effect measurements. Finally, it should be noted that the EQ moment of the 1174-keV state measured in this experiment is potentially a very useful probe for further measurements of this type in view of the long lifetime of that state and the large anisotropy of the cascade which decays through it. Thus, in this atom, an unusually broad range of interaction strength can be investigated using time-differential PAC.

ACKNOWLEDGMENTS

The authors are grateful to Professor M. E. Caspari for his invaluable support and encouragement. Dr. Hassa Bakhru and the staff of the Yale University Heavy Ion Linear Accelerator have been most cooperative in making their facilities available and in expediting the numerous irradiations required. Helpful conversations with Dr. W. E. Evenson and Dr. G. K. Shenoy about various aspects of the experiments and their interpretation are gratefully acknowledged, and thanks are due to Professor E. Bodenstedt, Professor E. G. Funk, and Dr. H. F. Wagner for communicating their results to us prior to publication.

APPENDIX

In this Appendix we present the results of a calculation of the perturbation factors $G_k(t)$ in polycrystalline sources for intermediate nuclear state spins $I=2$ and 3. In doing this we follow the formalism of Matthias, Schneider, and Steffen,¹⁷ who first included the effects of anisotropy of the EFG in such a calculation. These authors carried out calculations of $G_2(t)$ for $I=2$ and $\frac{5}{2}$, and $\eta=0, 0.2, 0.4$, and 1.0, in a local coordinate system³⁸ where $|V_{zz}| \geq |V_{yy}| \geq |V_{xx}|$. We have extended these calculations to the cases where $\eta=0, 0.1, 0.2$, and 0.4, for $k=2$, and $\eta=0, 0.1$, and 0.2, for $k=4$.

In the presence of asymmetry, the interaction Hamiltonian (1) is not diagonal in an $|Im_I\rangle$ representation, involving as it does terms in I_+^2 and I_-^2 . Before the perturbation factors can be calculated, the interaction matrix must be diagonalized. Once the eigenvectors $|n\rangle$ and eigenvalues E_n of the system are known, the perturbation factors can be calculated from the general expression for the perturbation factor in a polycrystalline source first given by Abragam and Pound.¹⁶ In the notation of Frauenfelder and Steffen,¹³

$$G_k(t) = \sum_{N, m_a, m_b; n, n'} (-1)^{2I+m_a+m_b} \\ \times \begin{pmatrix} I & I & k \\ m_a' & -m_a & N \end{pmatrix} \begin{pmatrix} I & I & k \\ m_b' & -m_b & N \end{pmatrix} \\ \times \langle n | m_b \rangle^* \langle n | m_a \rangle \langle n' | m_b' \rangle \langle n' | m_a' \rangle^* \\ \times \exp[(-i/\hbar)(E_n - E_{n'})t],$$

where the angular momentum factors are expressed in terms of $3j$ symbols in the normalization of Edmonds.³⁹ The terms $\langle n | m \rangle$ are the elements of the desired unitary transformation. The diagonalization cannot be made in closed form and thus must therefore be carried out numerically. A program for the diagonal-

³⁸ It should be noted that only in special cases involving lattices of rather high symmetry do these axes correspond to the local symmetry axes of the CEF. Thus, care should be taken in the application of these results.

³⁹ A. R. Edmonds, *Angular Momentum in Quantum Mechanics* (Princeton University Press, Princeton, N. J., 1960), 2nd ed.

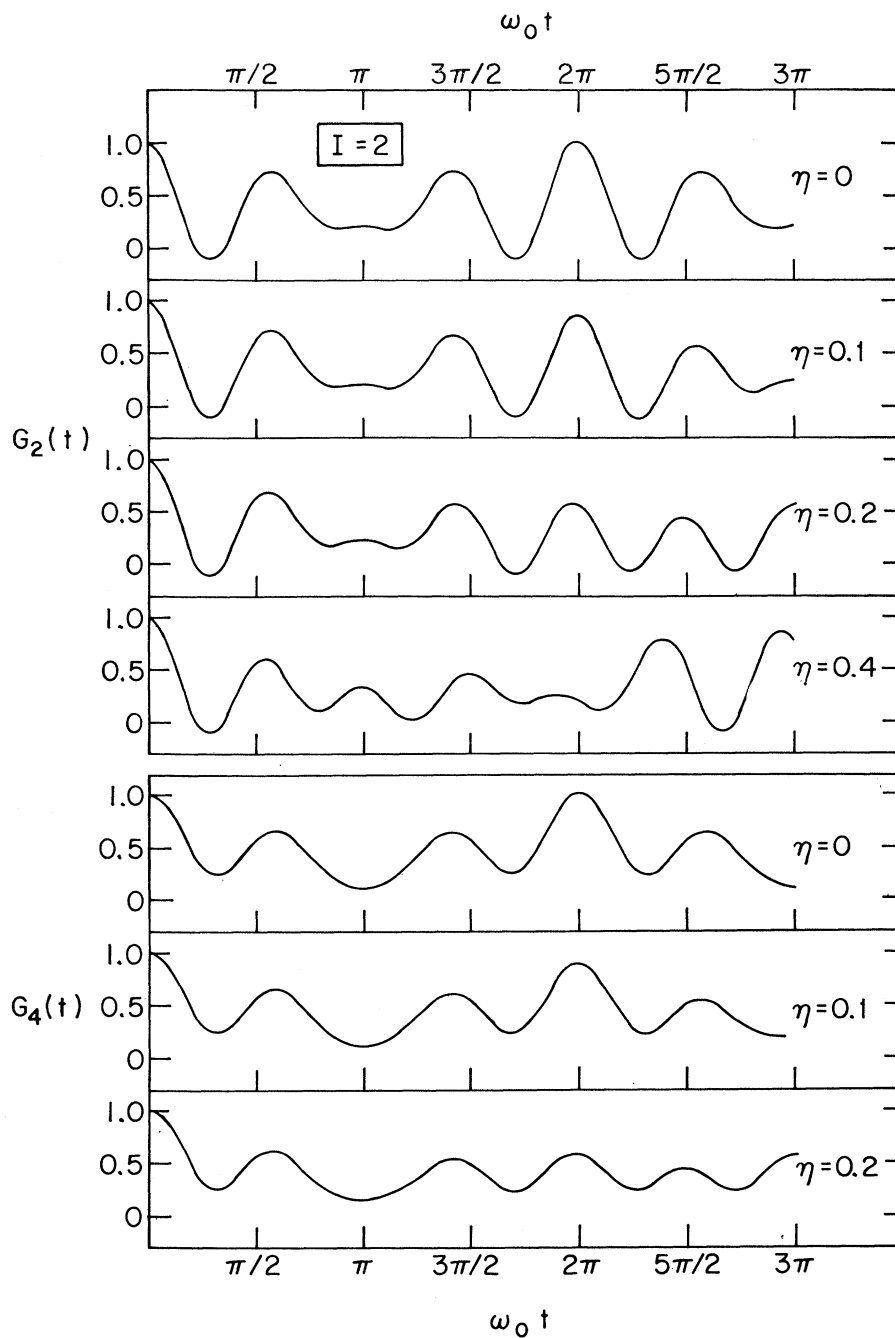


FIG. 6. Attenuation coefficients $G_2(t)$ and $G_4(t)$ for intermediate state spin $I=2$, calculated for various values of the asymmetry parameter η .

ization and calculation of the $G_k(t)$ was written in FORTRAN IV, and the calculations carried out on the IBM 360/75 computer at the University of Pennsylvania Computer Center.

Figures 6 and 7 show the calculated perturbation factors $G_2(t)$ and $G_4(t)$ for nuclear spin $I=2$ and 3, respectively. Those for $G_2(t)$, $I=2$ agree with the corresponding factors calculated by Matthias, Schneider, and Steffen.¹⁷ The general trend of the

effect of increasing asymmetry is the same in all cases: with increasing η the pattern becomes less regular. The loss of periodicity sets in faster as I and k increase, since a larger number of incoherent terms contribute to the sum in these cases. Thus the basic form of $G_k(t)$ is readily recognizable for $\eta=0.2$ with $I=k=2$, but is largely wiped out at the same asymmetry for $I=3$, $k=4$. It should be mentioned that, for the cases of interest in ^{172}Yb , the $k=4$ terms in the angular cor-

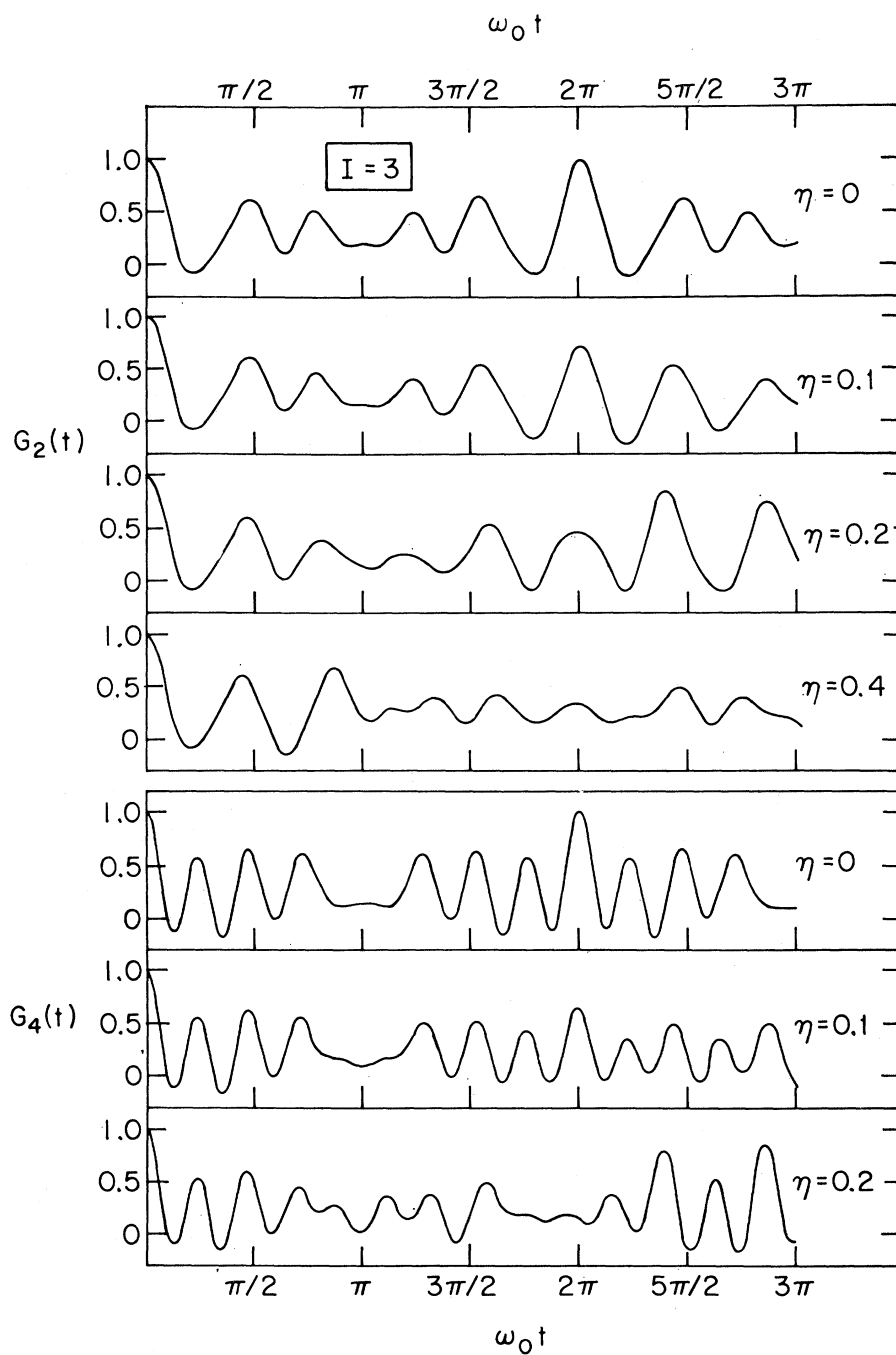


FIG. 7. Attenuation coefficients $G_2(t)$ and $G_4(t)$ for $I=3$, calculated for various values of the asymmetry parameter η .

relation function are negligible compared to the enormous $k=2$ terms. The results of the calculation show that the $G_2(t)$ are relatively insensitive to small ($\eta \leq 0.2$) deviations from axial symmetry. For quanti-

tative determination of η , it would appear that correlations with large $P_4(\cos\theta)$ contributions which depopulate through intermediate nuclear states with high spins are more appropriate.